Oxidation of hydrocarbon fragments on metal single crystals and on supported metals

F. Solymosi [*]

Institute of Solid State and Radiochemistry, A. József University and Reaction Kinetics Research Group of the Hungarian Academy of Sciences, [1] P.O. Box 168, H-6701 Szeged, Hungary

Abstract

Results obtained on the reactions of hydrocarbon fragments (methylene, methyl, ethyl, propyl and butyl) with adsorbed oxygen on metal surfaces are summarized and discussed. Hydrocarbon species have been generated by the thermal and photo-induced dissociation of corresponding iodo compounds or by the pyrolysis of azomethane. Methods used are X-ray and ultraviolet photoelectron spectroscopy, high resolution electron energy loss spectroscopy and temperature programmed desorption. It is shown that adsorbed oxygen atoms readily combine with C_xH_y fragments above 150 K, and pathways of the oxidation sensitively depend on the nature of the metals. © 1998 Elsevier Science B.V.

Keywords: Hydrocarbon; Oxidation; Metals

1. Introduction

In the last decade, our knowledge on the bonding, structure and reaction pathways of hydrocarbon fragments, C_xH_y, on well-oriented metal surfaces has been greatly improved, which is documented in several recent reviews [1–4]. There is no doubt that the work of Brian Bent significantly contributed to this knowledge. This progress is mainly due to the fact that several methods have been elaborated in the last decade to synthesize C_xH_y fragments of known composition on solid surfaces even at low temperatures.

After determination of the main features of the chemistry of C_xH_y species on various clean metal surfaces, attention was turned to their reactions with adsorbed oxygen atoms. As these reactions are the elementary steps in the partial oxidation of methane, it is expected that the results obtained may help to evaluate the mechanism of this oxidation process. In the present work, an account is given on the main features of the selective and complete oxidation of different C_xH_y species.

2. Methods for production of CH_x fragments

One possibility for the production of hydrocarbon fragments, C_xH_y, at lower temperatures is the thermal dissociation of corresponding

---

[*] Corresponding author.
[1] This laboratory is a part of the Center for Catalysis, Surface and Material Science at the József Attila University of Szeged.

halogenated hydrocarbons. The characteristic features of the adsorption and dissociation of these compounds on metal surfaces have been described in recent papers [1–8]. The gas phase carbon–halogen bond energies in alkyl halides are as follows: C–I, 55 kcal/mol, C–Br, 70 kcal/mol, C–Cl, 85 kcal/mol. In harmony with these data, the reactivity of alkyl halides with metals decreases in the order iodides > bromides > chlorides. As a result of this feature, mostly iodide compounds are used to generate hydrocarbon fragments on solid surfaces. The sensitivity of these compounds to illumination provides a possibility to produce C_xH_y fragments on metal surfaces even at ~ 100 K where the decomposition of C_xH_y can be excluded [4–8].

The dissociation of iodo compounds can be easily followed by X-ray photoelectron spectroscopy (XPS) via the binding energy (BE) of I(3d), as it differs by about 1.5–2.0 eV for molecularly adsorbed compounds and for atomically adsorbed iodine. Ultraviolet photoelectron spectroscopy (UPS) can be also used, but this method is less sensitive than XPS. High resolution electron energy loss spectroscopy (HREELS) is also applied in this area, as the characteristic vibrations of CH_xI_y and CH_x are different. In this case, the limited resolution of HREELS may cause a problem.

Recently, Peng et al. [9] and Jenz et al. [10] described a methyl radical source for use in high vacuum. Methyl radicals are generated through azomethane pyrolysis in a tubular reactor located inside an ultrahigh vacuum chamber. Methyl yields as high as 42% have been achieved. By means of this method, almost pure adsorbed CH_3 layer can be produced on the solid surfaces. Other gases formed during the pyrolysis or in the reaction of methyl radicals on the walls of the reactor include nitrogen, methane, ethane and hydrogen. From these gases, hydrogen is the less desired product. In contrast to halogen atoms, it reacts readily with adsorbed methyl groups at relatively low temperature.

In the case of the generation of methylene, CH_2N_2 is also used [11]. This compound is the best source of CH_2 as only N_2 and CH_2 are produced in its low-temperature dissociation. The explosive nature of this compound, however, makes its application less attractive.

3. Oxidation of C_xH_y on metal single crystals

3.1. Oxidation of CH_2

3.1.1. Rhodium

Methylene species was produced by the dissociation of adsorbed CH_2I_2. The study of the interaction of CH_2I_2 with clean Rh(111) revealed that the cleavage of C–I bond in the monolayers proceeds at 170–220 K [12]. The main product of the reaction of CH_2 on Rh(111) is CH_4 which evolved at 200–300 K. The coupling of CH_2 into C_2H_4 was very limited. Determination of the XPS signal for $I(3d_{5/2})$ at 620.0–620.4 eV suggests that the uptake of CH_2I_2 on an oxygen-dosed Rh(111) surface is not influenced up to $\theta_O = 0.3$, but decreases by about 20–25% at higher oxygen coverages [12,13]. While on a clean surface, spectral changes in XPS are indicative of the dissociation of molecularly adsorbed CH_2I_2 started at 173 K, and was completed at 219 K, in the presence of preadsorbed oxygen ($\theta_O = 0.3$–0.5), these values were shifted to ~ 200 and 250 K, respectively. The main products of the reactions of CH_2 on clean Rh(111) were also identified in the presence of adsorbed O atoms. The peak temperature for CH_4 desorption ($T_p = 240$ K), and the area of the CH_4 peak, remained practically unaltered up to $\theta_0 = 0.3$. Above this oxygen coverage, less CH_4 was formed and its T_p was shifted to the higher temperature of 260 K. New products were CH_2O ($T_p = 280$ K), CO_2 ($T_p = 410$ K) and H_2O ($T_p = 415$ K). Some TPD curves are presented in Fig. 1. Formation of CH_2O was observed at the lowest oxygen coverage used, $\theta_O = 0.07$. Its evolution started above 170 K and reached a maximum at 230 K.
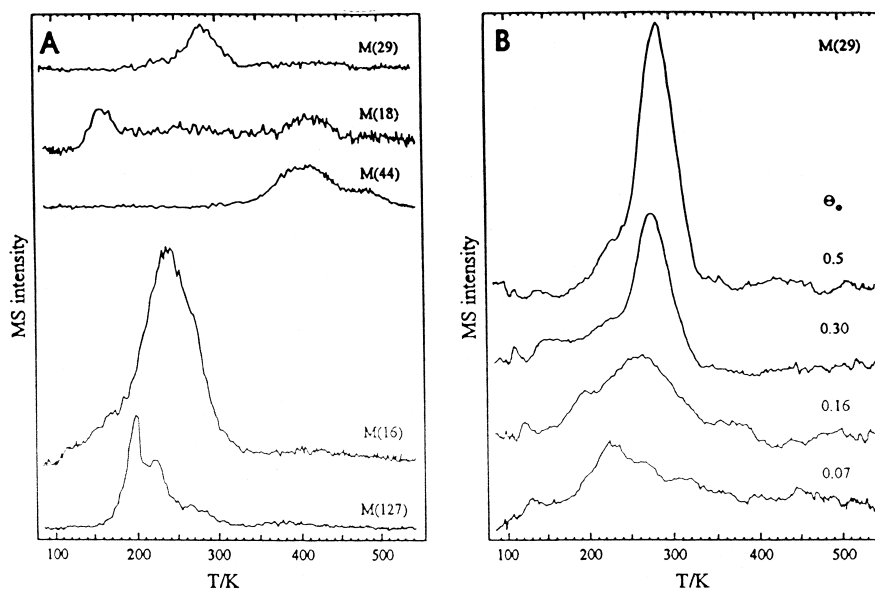
Fig. 1. (A) TPD spectra following CH_2I_2 adsorption on a clean and oxygen-dosed Rh(111) ($\theta_O = 0.3$) at 90 K. (M(29) CH_2O; M(18) H_2O; M(44) CO_2; M(16) CH_4; M(127) I). (B) Effects of oxygen coverage on the formation of CH_2O following CH_2I_2 exposure on oxygen-dosed Rh(111) at 90 K [12].

These values shifted to higher temperature as θ_O was increased. The highest peak temperature for CH_2O evolution was 280 K. An increase in the O coverage enhanced the production of H_2O and CO_2. These two compounds desorbed in the same temperature range with a constant peak temperature of 410–415 K. Taking into account the areas of TPD peaks for different products, it was found that at $\theta_O = 0.3$ the ratios for CH_2O/CO_2, CH_2O/CH_4 and CO_2/CH_4 were 0.25, 0.06 and 0.22, respectively. This suggests that the reactions of adsorbed CH_3 (formation of CH_4) observed for a clean surface, occurs for O-dosed Rh(111) to a significant extent.

In a search for new surface compounds, HREELS measurements were carried out under similar conditions. The adsorption of CH_2I_2 on oxygen-dosed Rh(111) at 90 K yielded very similar spectra as those obtained for the clean surface. Independently of the oxygen coverage, the characteristic losses of adsorbed CH_2O determined earlier [14,15] were absent. There was no spectral indication of other new surface complexes either.

In light of these features, we can state that at low oxygen coverages the main reaction channel for CH_2 is still its self-hydrogenation (with the possible participation of background hydrogen), as indicated by the unaltered production of CH_4. Parallel with this, a fraction of CH_2 formed in the dissociation of CH_2I_2 interacts with adjacent adsorbed oxygen atoms to give CH_2O, which desorbs promptly after its formation, without appreciable oxidation. Its formation is undoubtedly a reaction-limited process. If this assumption is correct, then the illumination of the adsorbed layer at 90 K may produce CH_2O around this temperature, as the illumination of adsorbed CH_2I_2 on the Rh(111) surface induces the production of CH_2 through the dissociation of CH_2I_2 even at 90–100 K [12,13]. In harmony with this, the formation of CH_2O was identified above 110 K by means of the post-irradiation TPD measurements.

The total oxidation of CH_2 proceeds at much higher temperatures (above 340 K) to give gaseous CO_2 and H_2O. We found no indications of the presence of these compounds in the

HREEL spectra, which is not surprising, as CO_2 desorbs from clean Rh(111) with $T_p = 250$ K [16] and H_2O does so with $T_p = 158$ and 183 K [17,18]. As regards to the formation of these products, there are several possible reaction channels. Most probable is that the oxidation occurs through the formation of formate species, HCOO, which decomposes to CO and H. Formate can exist only transitorily on the Rh surface, as the HREEL spectra did not indicate its presence at all. This is consistent with the finding that formate decomposes on Rh(111) between 200 and 250 K [19]. An alternative route involves the oxidation of CH formed in the decomposition of adsorbed CH_2 above 350–400 K.

In order to prove further that CH_2 is a key species in the formation of CH_2O and in the complete oxidation reactions, the effects of adsorbed oxygen on the CH_2Cl_2/Rh(111) system was examined [13]. In contrast with the iodo compound, CH_2Cl_2 adsorbs molecularly at 90 K and undergoes only a limited dissociation (less than 15%) during annealing. By means of TPD, we detected the formation of a small amount of CH_4 with $T_p = 200$ K. In the HREEL spectrum, only the characteristic losses of the molecularly adsorbed compound were identified. The same features were observed following adsorption and annealing on an oxygen-dosed Rh(111) surface. No traces of CH_2O in the temperature range 90–300 K was found. However, when the coadsorbed layer had been illuminated for 60 min at 90 K, which induced the dissociation of CH_2Cl_2, the evolution of CH_2O occurred in the post-irradiation TPD at around 230 K.

Similar results on the $CH_2 + O$ reaction were reported by Bol and Friend [20,21]. They also observed the retarding effect of coadsorbed O on the cleavage of C–I bond. The minimum temperature required for C–I bond breaking increases from 150 K (clean surface) to 200 K on Rh(111)–(2×2)–O and 300 K on Rh(111)–p(2×1)–O [20,21]. The relative yields of various products sensitively depends on the O-

coverage. At the highest oxygen coverage formaldehyde formation is the dominant pathway. As regards to the formation of CH_2O, their view differs from that described above. They proposed that the addition of oxygen to nascent CH_2 is the pivotal step in the production of formaldehyde. They argue against the reaction between adsorbed CH_2 formed in the dissociation of CH_2I_2, and surface oxygen atoms. This is based on their observation that following annealing a 75% of saturation coverage of CH_2I_2 to 220 K followed by O_2 exposure on this surface at 100 K did not yield any formaldehyde. Although HREEL spectra showed that $O_{(a)}$ is formed on Rh(111) covered by the products of CH_2I_2 dissociation, the open questions are whether the O atom coverage attained in this way is sufficient for detectable CH_2O production, and whether the position of adsorbed O is favourable for this reaction.

There are several ways to obtain further evidences for the mode of the combination of CH_2 and adsorbed O atoms. One of them is to develop a method for production of gas-phase CH_2 and adsorb on clean and O-dosed surfaces. Another possibility is the complete photolysis of the adsorbed CH_2I_2 on clean Rh(111) ~ 100 K, which provides only CH_2 without its decomposition products. Experiments are in progress in our laboratory in both directions.

3.1.2. Palladium

The inhibiting effect of preadsorbed oxygen on the dissociation of CH_2I_2 was also observed on Pd(100) [22]. As a result, the temperature of the self-hydrogenation of CH_2 to CH_4 was shifted from 255 K (clean Pd) to 265 K (O-dosed Pd, $\theta_O = 0.5$). A significant decrease in the amounts of CH_4 and C_2H_4 production was also experienced. The new products formed on oxygen-dosed Pd(100) are CH_2O ($T_p = 247$ K), CO ($T_p = 430$ K), CO_2 ($T_p = 275$ K). Formation of CH_2O was observed at the lowest oxygen coverage, at $\theta_O = 0.125$, used in the work. Its production started above 150 K and reached a maximum at 220 K. The latter value shifted to

higher temperature, up to 247 K, as θ_O was increased. The amount of CO_2 and H_2O formed increased almost linearly with the increase of the oxygen coverage. As regards to the CO_2/CH_4, CH_2O/CH_4, CH_2O/CO_2 ratios at $\theta_O = 0.5$, the following approximate values: 2.0, 0.17 and 0.08 were calculated.

In a search of new surface compounds, UPS measurements were carried out under similar conditions. The adsorption of CH_2I_2 on O-dosed Pd(100) at 90 K yielded very similar spectra as those obtained for the clean surface [23]. Annealing the coadsorbed layer, weak photoemission signals were observed at 8.4 and 10.6 eV, which were due to the adsorbed CO (Fig. 2). Weak photoemission lines characteristic for undissociated CH_2I_2 were also present up to 359 K. There was no spectral indication of the presence of adsorbed CH_2O or H_2CO_2 at any temperature. Accordingly, similar to Rh(111), the CH_2 species combines readily with the adsorbed oxygen atoms on Pd(100) to give CH_2O, which desorbs promptly after its formation. Taking into account the instability of CH_2O on Pd(100) surface [24], as well as the UPS results, it was concluded that its release is a reaction

limited process. The significant reduction of methane and ethylene formation on the oxygen-dosed surface is no doubt due to the competing process of the reaction of CH_2 with adsorbed O atoms. The presence of adsorbed oxygen may also hinder the diffusion of CH_2, which contributes to the decrease of the probability of CH_2 coupling.

The evolution of H_2O above 200 K with $T_p = 275$ K (which is only slightly higher than the recombination temperature of OH groups, $T_p = 248–256$ K, on Pd(100) surface [25,26], suggests that the total oxidation of CH_2 also occurs at this temperature. This may proceed through the oxidation of CH_2O and/or through transient formation of other surface intermediates. As CO_2 does not adsorb on clean Pd(100) surface under UHV conditions even at 90 K [27], the formation of CO_2 ($T_p = 430$ K) is no doubt a reaction limited process. Since the release of CO_2 is not accompanied by the evolution of other products (H_2O, H_2), we can exclude the possibility that it is the result of the decomposition of CH-containing surface compounds, for instance, formate species. It is more likely that, in consistence with the UPS spectra-adsorbed CO is formed in the surface reaction, which is oxidized to CO_2 above 350 K.
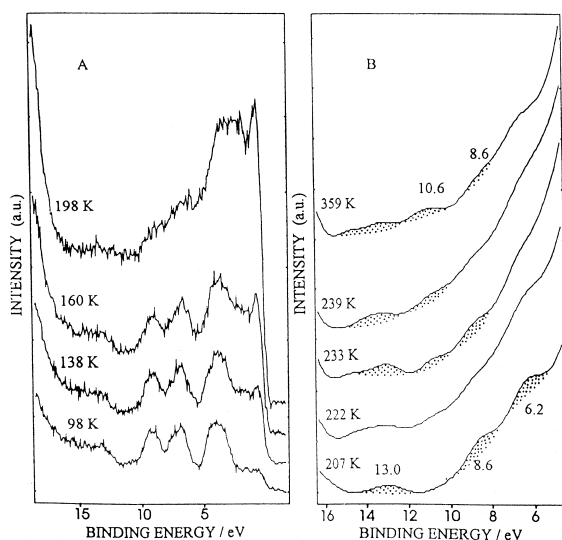
3.1.3. Platinum

The reaction of $CH_2(a)$ with adsorbed O atoms has been first investigated by Berlowitz et al. [28]. CH_2 was produced by the thermal dissociation of CH_2N_2 at ~ 100 K. Product characteristics of the clean surface were observed together with the oxidation products, H_2O, CO and CO_2. No formaldehyde was detected. They assumed that the oxidation of CH_2N_2, C_2H_2 and C_2H_4 on Pt(111) proceeds via the same rate-controlling intermediate and suggested that either $C_2H_x(a)$ (which forms from the recombination of $CH_2(a)$ before oxidation occurs) or CH(a) was involved.

In contrast to this work, the formation of formaldehyde was observed from $ClCH_2I$ reac-

Fig. 2. UPS spectra for adsorbed CH_2I_2 on oxygen-dosed Pd(100) surface at 98 K, and after annealing (B for difference spectra) [22].

tion on O-covered Pt(111), which was actually the first positive result on the coupling of CH_2 and O [29]. This finding led the authors to believe in the key promotion role of coadsorbed halogens [29]. In this case, a reaction between adsorbed CH_2 and surface oxygen was also assumed to occur; the process between gaseous CH_2 and adsorbed O was not considered.

Since no O-containing reaction intermediates associated with the oxidation products were identified by HREELS, it was concluded that the evolution of the O-containing compounds is reaction limited and involves CH_2(a) and CH_2Cl(a). Another point is that dissociation of C–I and C–Cl and the formation of CH_2O proceed simultaneously. It was proposed that CH_2O(a), in di-σ-bonded form, $-CH_2O-$, is the key intermediate that leads to formaldehyde, CO and CO_2. The distribution of these products is determined by the local oxygen and halogen coverages. Adsorbed halogens, by modifying the surface, may play an important role in the evaluation of CH_2O, as CH_2O normally adsorbs dissociatively on Pt(111) to give CO and H at 105 K.

3.1.4. Copper and silver

The reaction of CH_2 with adsorbed O atoms has been investigated on Cu(100) surface [30]. The reactivity of clean Cu is basically different from that of Pt metals, as CH_2 is coupled readily into ethylene which desorbs ($T_p = 240$ K) instead of decomposition and self-hydrogenation [30–34]. The formation of a strongly bound di-δ-bonded ethylene was also detected, which transformed into ethylidyene, CCH_3 at 371 K.

XPS measurements demonstrated that the uptake of CH_2I_2 on oxygen-dosed Cu(100), $\theta_O = 0.5$, at different CH_2I_2 exposures is practically the same as for the clean surface [30,31]. A shift in the binding energy of $I(3d_{5/2})$ to lower energy, indicating the cleavage of the C–I bond, occurred at higher temperature compared to a clean surface. At $\theta_O = 0.5$, the temperature of the completeness of the dissociation was 268 K,

which is about 60 K higher than that for the clean Cu(100).

TPD spectra showed that with the increase of the O coverage, the amount of ethylene desorbed and its T_p values markedly decreased, and above $\theta_O = 0.12$ no or very little ethylene desorption was found [30,31]. At the same time, H_2O ($T_p = 344$ and 460 K) and CO_2 ($T_p = 550$ and 602 K) are produced. H_2CO was detected only in traces. This suggests that the reaction pathway of CH_2 on O-dosed Cu(100) is basically different from that established for Rh and Pd surfaces. It appears that the thermodynamic driving force for the coupling of CH_2 formed above 200 K on Cu(100), is still greater than that for the combination of CH_2 with adsorbed O atoms. As no desorption of C_2H_4 was measured above $\theta_O \sim 0.12$, it was assumed that the ethylene and/or ethylidyene formed interacted strongly with adsorbed O atoms resulting in surface compounds the oxidation of which occurred above 300 K.

Completely different picture was obtained following the irradiation of the coadsorbed layer, which induced a complete dissociation of CH_2I_2 even at 100 K [30]. In this case, the evolution of CH_2O with a $T_p = 280$ K was observed. Its amount increased with the rise of O coverage. At the same time, the peak temperature of CO_2 shifted to lower temperature, 468 K, which agrees well with the T_p values for CO_2 evolution from $CH_2O + O/Cu(111)$ and $HCOO + O/Cu(111)$ systems [35,36].

In the interpretation of these new features, the significant difference between dark and photo experiments should be stressed. In the latter case, CH_2 species is formed already at 100 K, whereas in dark experiment this occurs only above 200 K. Accordingly, the coupling of CH_2 at 100 K is restricted, and instead CH_2 species combined with O atoms to give CH_2O. A fraction of CH_2O desorbs above 200 K, another fraction is oxidized to formate, which releases H_2 and CO_2 at 468 K. As the formation of C_2H_4 is limited, consequently the products of its further reactions (transformation into

ethylidyene, oxidative dehydrogenation, etc.) are minimal. Experiments are in progress to exploit further details of the reaction of CH_2 with adsorbed oxygen on Cu surfaces.

Different results were obtained on Ag(111) surface [37]. The dominant pathway of the reaction of CH_2 (produced by the dissociation of CH_2I_2) on clean Ag(111) is also its coupling into C_2H_4. In the presence of adsorbed oxygen, however, CH_2O ($T_p = 180–275$ K), CO_2 ($T_p > 550$ K) and H_2O ($T_p = 160–180$ K) were produced. Ethylene evolution at saturation oxygen coverage, $\theta_O = 0.4$, was not detected.

3.2. Oxidation of CH_3

3.2.1. Rhodium

In the study of the oxidation of CH_3 on Rh(111), it was observed that preadsorbed O atoms shifted the temperature of the complete dissociation of CH_3I from 200 K to 275 K [38,39]. This is demonstrated by XP spectra presented in Fig. 3. TPD measurements showed the formation of new products, CO_2 ($T_p = 450$ and 500 K), CO ($T_p = 520$ K) and H_2O ($T_p = 415$ K) which suggests that CH_3 undergoes oxidation between 400 and 500 K. The products of oxidation gradually increase in amount with

the oxygen coverage. Note that CH_2O has not been identified in the desorbing products. An attempt was also made to detect CH_3OH, C_2H_6 and C_2H_4 without any positive result. The effect of preadsorbed oxygen is also manifested in the reactions of CH_3 observed for the clean surface: its self-hydrogenation into methane occurred in a wider temperature range than on the oxygen-free surface, and a significant portion of methane evolved only above 200 K. This suggests a certain stabilization of CH_3 species. Analysis of TPD results shows that at $\theta_O = 0.4$ about 77% of the CH_3 species have been oxidized, and 23% have been converted into CH_4.

In a search for surface intermediates in the oxidation reaction, HREELS measurements were carried out under similar conditions [39]. Spectra are displayed in Fig. 4. The losses obtained for O-covered Rh(111) corresponded well to the molecularly adsorbed CH_3I. The characteristic losses of adsorbed CH_3I and CH_3 on Rh(111) and their assignment are given in Table 1. On warming the adsorbed layer to 150–180 K, a new feature appeared at 1040–1050 cm^{-1}, which was eliminated at 185–200 K. Further changes occurred above 220 K: the losses of adsorbed CH_3I attenuated, and new peaks developed at 2920–2930 cm^{-1} (ν_{as} CH_2), 2020–
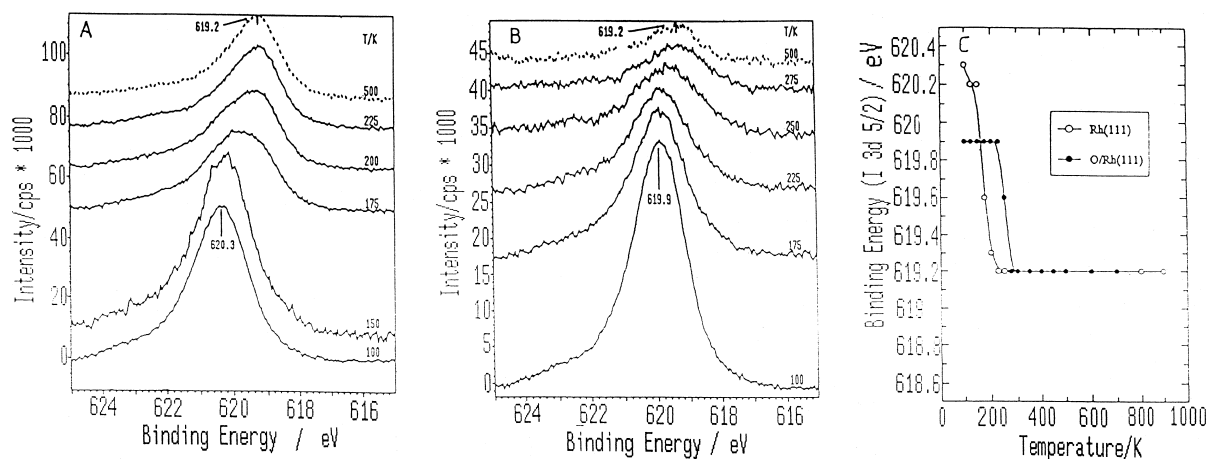

Fig. 3. Effects of annealing on the I($3d_{5/2}$) XP spectra of adsorbed CH_3I on (A) clean and (B) oxygen-dosed Rh(111) ($\theta_O = 0.4$), and (C) on the position of the I($3d_{5/2}$) peak [39].
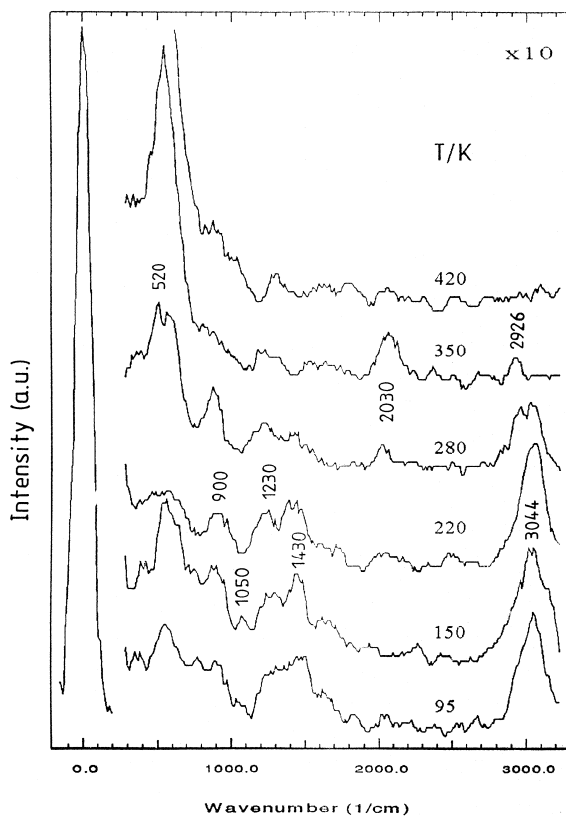
Fig. 4. HREEL spectra of adsorbed CH_3I on oxygen-covered Rh(111) ($\theta_O = 0.4$) after annealing at different temperatures [39].

2030 cm^{-1} (νCO) and 520 cm^{-1} (νC–I) [39]. At 310–350 K, the dominant losses were at 2926 and 2040–2050 cm^{-1}. The loss at 520 cm^{-1} became stronger. These peaks vanished (with the exception of the 520 cm^{-1} loss) by warming the adsorbed layer to 420 K.

Table 1
Vibrational frequencies of CH_3I and CH_3 (cm^{-1}) and their assignments [38]

| Vibrational modes	$CH_3I(g)$	CH_3I/Rh(111)	CH_3/Rh(111)
ν_a (CH_3)	3060		2920
ν_s (CH_3)	2933	3044	
δ_a (CH_3)	1436	1430	1350
δ_s (CH_3)	1252	1230	1185
ρ (CH_3)	882	900	760
ν (C–I)	533	522	

The obvious first step in the oxidation reaction is the selective addition of oxygen atoms to adsorbed CH_3 to yield methoxy species

$$CH_3(a) + O(a) = CH_3O(a)$$
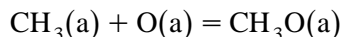
similarly as in the case of the $CH_2 + O$/Rh(111) system. In the HREEL spectra, however, we found only a very weak, but reproducible loss at 1040–1050 cm^{-1} which can be attributed to the C–O stretch in methoxy species. This loss appeared at 150–180 K, but was not discernible above 200 K. The weak signal of methoxy species may be associated with the fact that at 150–180 K we can expect only a very limited dissociation of adsorbed CH_3I. The combination of CH_3 with adsorbed O atoms was described in Scheme 1. The important feature of this scheme is the interaction of the CH_3 of the adsorbed CH_3I with O atoms before the rupture of the C–I bond. The reaction of CH_3I with surface oxygen to yield methoxy is not unique, as it was also observed following the adsorption of CH_3I on Al_2O_3 [40].

The fact that the feature at 1040–1050 cm^{-1} was not detectable in the high temperature region (where the dissociation of CH_3I is more extended) is not in contradiction with this picture, if we take into account the low stability of methoxy species on the Rh(111) surface [41–43]. Following the adsorption of CH_3OH on clean Rh(111), where the surface concentration of methoxy species was obviously high, the losses due to methoxy species were identified only up to 180 K [41].

The observation that the peak temperatures of the production of H_2O, CO and CO_2 in the present case approach those measured following the adsorption of CH_3OH on oxygen-dosed Rh(111) (T_p (H_2O) = 375 K, T_p (CO) = 510 K, T_p (CO_2) = 450 K) provides further evidence
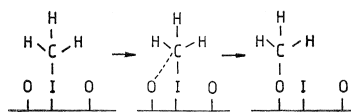
Scheme 1.

that the oxidation of CH_3 occurs through the transient formation and reactions of methoxy species [42]. These reactions may involve the decomposition of CH_3O

$$CH_3O(a) = CO(a) + 3H(a)$$

and the oxidation of adsorbed CO and H, and/or the direct oxidation of CH_3O to H_2O and CO_2. Note that following the adsorption of CO_2 and H_2O on a Rh(111) surface, CO_2 desorbed with $T_p = 250$ K [44] and H_2O did so with $T_p = 158$ and 185 K [45,46].

The reaction of methyl radicals and surface oxygen also on Rh(111) has been also studied by Bol and Friend [47]. In this case, CH_3 radicals were generated by pyrolysis of azomethane. Adsorbed methyl and methoxy were detected by means of HREELS following exposure of oxygen-covered Rh(111) to methyl radicals for all combinations of methyl (0.1–0.25 monolayers) and oxygen (0.2–0.5 monolayer) coverages studied. CO ($T_p = 440$ K), CO_2 ($T_p = 400$ K) and a small amount of formaldehyde around 290 K were identified in the desorbing products. It was an important observation that methoxy was not produced when methyl was adsorbed on clean Rh(111) first and followed by oxygen adsorption.Therefore, they assumed that carbon–oxygen bonds are formed in the direct reaction of methyl radicals with surface oxygen on Rh(111)–p(2×1)–O at 100 K.

In the above considerations, several arguments have been presented to explain the low intensity of methoxy at low temperatures and its absence at high temperatures. An alternative interpretation is that the above route represents only a minor pathway in the oxidation of CH_3 species: the dominant process is the direct abstraction of hydrogens of CH_3 by adsorbed oxygen to give initially adsorbed OH and surface C. The oxidation of surface carbon on Rh, however, proceeds only above 550–600 K [48,49]. The peak temperatures of CO_2 evolution on Rh(111) are 660 and 750 K [49], which are considerably higher values than those determined for the production of CO and CO_2 in the

present study. This makes the alternative route of the oxidation less likely.

3.2.2. Palladium

In the oxidation of methyl on Pd(100), the formation of CH_2O ($T_p = 270$ K), CO ($T_p = 460$ K), CO_2 ($T_p = 440$ K) and H_2O ($T_p = 295$ K) were established [22]. The surface reactions occurring in the coadsorbed layer were also followed by HeII photoelectron spectroscopy, but no spectroscopic evidence for the transitory existence of methoxy species was obtained. This is not surprising as the formation of CH_3 and its oxidation start above 180–200 K, where according to previous measurements CH_3O decomposes rapidly to adsorbed H and CO on Pd(100) surface [50–52]. In the presence of adsorbed oxygen atoms these adsorbed species are oxidized at higher temperatures to yield H_2O and CO_2. Their formations are no doubt reaction limited processes.

3.3. Oxidation of C_2H_5

In the presence of preadsorbed oxygen the formation of both ethylene and ethane, the products of the reaction of C_2H_5 species on Rh(111) [53,54], shifted to higher temperatures,very likely due to the delayed dissociation [39]. In addition, the amount of ethane significantly decreased. The possible reason is that the hydrogen formed in the dehydrogenation of C_2H_5 reacted with adsorbed oxygen atoms to give H_2O. The release of H_2O at 260–360 K can be attributed to this process.

The oxidation of the C_2H_5 species also occurred in the adsorbed layer as indicated by the formation of H_2O, CO and CO_2 at higher temperature, $T_p(H_2O) = 320$ and 420 K, $T_p(CO_2) = 450$ and 500 K, $T_p(CO) = 500$ K. These temperature values are practically the same as found in the complete oxidation of CH_3 species. In addition, the evolution of acetaldehyde ($T_p = 340$ K) was also established.

It was assumed that the oxidation of adsorbed ethyl proceeds in a similar way as described for

the oxidation of adsorbed methyl species, i.e., through the interaction of the C_2H_5 group of adsorbed C_2H_5I with oxygen atoms, and the transient formation and reactions of adsorbed ethoxy species [39]. The fact that the ethoxy intermediate did not accumulate on the surface in a detectable amount at the temperature of oxidation reaction is probably associated with its low thermal stability. Adsorbed C_2H_5O decomposes completely on the Rh(111) surface to H and CO below 250 K [55]. The formation of acetaldehyde was assumed to occur via β-hydrogen elimination of adsorbed ethoxy, as was established by Hautman and Barteau [55].

A more detailed study performed by Bol and Friend [56] discovered several new features on this system. It appeared that the product distribution of the oxidation of C_2H_5 sensitively depends on the oxygen coverage. This is shown in Fig. 5. The more fully oxidized products, CO and CO_2, are formed at low-to-intermediate oxygen coverages, whereas the partial oxidation
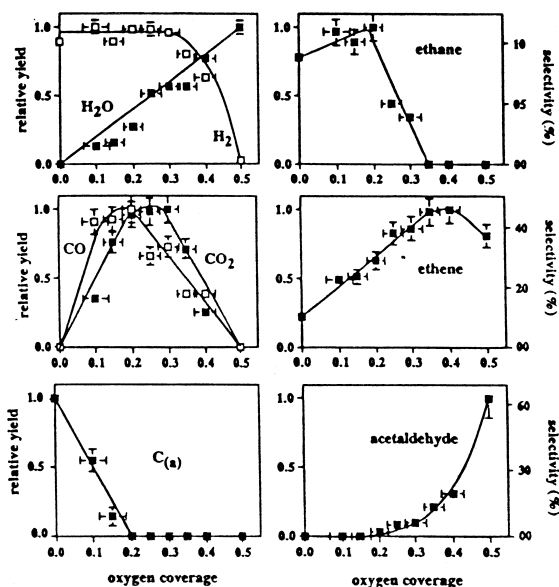
product, acetaldehyde, is produced at high oxygen coverage. The oxidation of C_2H_5 to acetaldehyde with a selectivity of 62% occurred. The peak temperature of acetaldehyde evolution was 355 K. The formation of C_2H_4 and H_2O was the competing pathway. No CO or CO_2 was formed at this oxygen coverage.

The predominance of CO production at low oxygen coverages was attributed to the C + O reaction. The increase in the selectivity for CO_2 vs. CO production was explained with an increase in the probability of carbon reaction with two oxygens on the surface. Unfortunately, the authors did not report the desorption temperatures of CO and CO_2. Therefore, their assumption cannot be critically evaluated. As was mentioned before the reaction between C and O on Rh(111) proceeds at very high temperature. This interpretation was based on the assumption that on clean Rh(111) nonselective decomposition of C_2H_5 to H_2 and adsorbed C is the dominant pathway, which is in contrast to the results obtained on the reaction of C_2H_5 on clean Rh(111), where the main products were C_2H_4 and C_2H_6 [53].

The oxidation of ethyl species has been described by the scheme shown in Fig. 6. It was assumed that the rate determining step is the breakage of intact C_2H_5–I. An interesting feature of this scheme is that the dissociation of C_2H_5I occurs on the free Rh sites, and that no interaction of C_2H_5I with adsorbed O is proposed. In contrast, it is assumed that gaseous C_2H_5 radicals formed in the dissociation of C_2H_5I interacts with adsorbed O atoms. However, spectroscopic identification of the transient ethoxy intermediate formed during the reaction was not possible because the C–H bonds at the position adjacent to the oxygen are rapidly cleaved, affording acetaldehyde and acetone at the temperature required for C–I bond breaking.

Fig. 5. Relative yields of H_2, H_2O, CO, CO_2, adsorbed C, ethene, ethane, and acetaldehyde and selectivities for ethene, ethane, and acetaldehyde formation in the reaction of ethyl on oxygen-covered Rh(111) as a function of the oxygen coverage. The yields are normalized for the total amount of ethyl iodide reacting [56].

3.4. Oxidation of C_3H_7

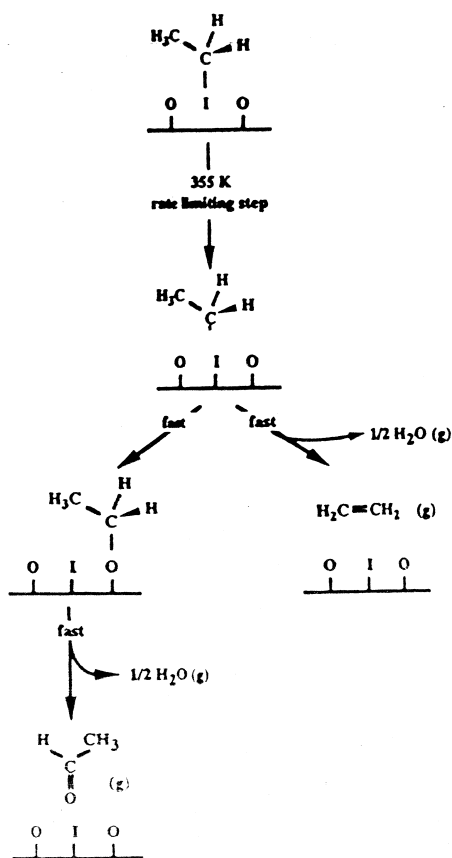Bol and Friend [56] also studied the oxidation of 2-propyl on Rh(111) surface using 2-propyl

Fig. 6. Schematic of proposed mechanism for the oxidation of ethyl iodide on Rh(111)–p(2×1)–O [56].

2-propyl has been described in the same way as that of ethyl species (see scheme in Fig. 6). Spectroscopic identification of the transient 2-propoxy intermediate was not successful.

Different results were obtained for the oxidation of 2-propyl on oxygen-dosed Ni(100) [57]: partial oxidation was favored at low oxygen coverages and total oxidation on oxide films. Annealing the 2-propyl iodide adsorbed on O–Ni(100) between 120–200 K caused the rupture of the C–I bond and the generation of the 2-propyl-group on the Ni sites. For submonolayer oxygen coverages, the 2-propyl groups undergo hydrogenation–dehydrogenation to form propane, propene and hydrogen. If propyl species is formed near oxygen sites, it migrates and reacts to give 2-propoxide groups. The propoxide moiety was found to be stable on the surface up to 325 K, where it undergoes β-hydride elimination to give acetone. It was also observed that propene does not react to yield acetone on O-dosed Ni(100).

3.5. Oxidation of t-butyl

Following the adsorption of t-butyl iodide on Rh(111)–p(2 × 1)–0, the formation of t-butanol, isobutene and water, along with trace amounts of CO and CO_2 were observed at 260 K [58]. Water and t-butanol were also produced in peaks at 390 K with small amounts of isobutene and water. Vibrational studies indicated that the C–I bond in t-butyl iodide remained intact up to the onset of product formation, based on the persistence of the δ(C–C–I) and ν(C–I) modes at 250 and 465 cm^{-1}, respectively. It is assumed that t-butyl radical formed in the C–I bond cleavage rapidly reacts with oxygen atoms producing adsorbed t-butoxide. The formation of this species was inferred from the development of a peak at 745 cm^{-1}. However, the contribution from other modes involving the hydrocarbon framework was not excluded. Isotopic labelling for a more definitive assignment is clearly needed. Some of the t-butoxide formed reacted with the hydrogen produced in the β-

iodide as a source of C_3H_7. Similarly, as in the case of C_2H_5, at saturation O coverage ($\theta_O = 0.5$) no CO and CO_2 were detected: the main reaction products were acetone, propene and H_2O, all evolving at 335 K. The acetone and propene peaks have essentially the same line shape, suggesting that they are formed from the same intermediate and via the same rate-limiting step.

At lower oxygen coverages CO, CO_2, H_2 and C_3H_8 were observed. Concomitantly, the acetone production diminished nearly when the initial oxygen coverage was 0.25 or lower. Note that on the clean surface the decomposition of C_3H_7 to gaseous H_2 and surface C predominated; some propene and trace amounts of propane were also identified. The oxidation of

hydride elimination step to yield gaseous *t*-butanol at 260 K. Decomposition of transient *t*-butoxide is probably responsible for the production of isobutene.

3.6. Oxidation of CH_x fragments on supported metals

There are very few studies on the oxidation of CH_x fragments on supported metals. The first attempt to add oxygen to CH_x species on Pd/SiO_2 did not lead to a positive result [59]. The possible reason is that the metal content was too low to detect any reaction of metal surfaces. Driessen and Grassian [60] were more successful. They studied the oxidation of CH_3 on Cu/SiO_2 using FTIR spectroscopy. The metal content was $\sim 15\%$. Following the adsorption of CH_3I on oxidized Cu/SiO_2 at 300 K, they observed a very complex spectrum containing several bands in the CH stretching region (2700 to 3200 cm^{-1}) and in the region extending from 1350 to 1600 cm^{-1} (Fig. 7). The observed bands and their assignments are listed in Table 2. It is important to point out that adsorption of CH_3I on pure silica at 300 K gave no absorption bands. In the analysis of the spectra they claimed the presence of methoxy,
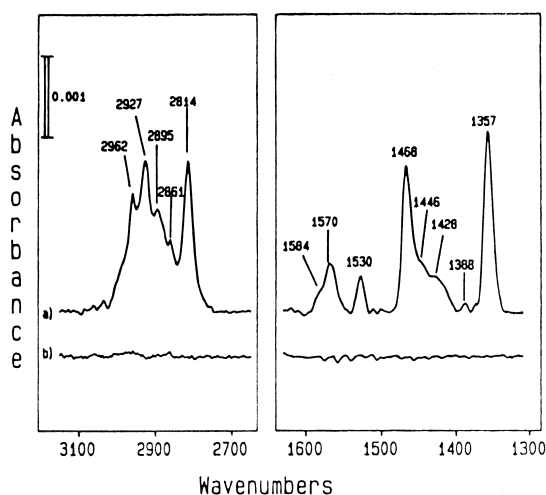
Table 2

Vibrational frequencies (cm^{-1}) of adsorbed methoxy species and their assignments [60]

Vibrational modes	Cu/SiO$_2$[a]	Cu(110)[b]
ν_{as} (CH$_3$)	2927	2940
ν_s (CH$_3$)	2814	2840
ν_{as} (CH$_3$)	2895	
δ (CH$_3$)	1468	1460

[a] Methoxy species formed following the adsorption of CH_3I on an oxidized Cu/SiO_2. Other bands appeared in the IR spectrum (Fig. 7) were attributed to bidentate formate.
[b] Methoxy species formed following the adsorption of CH_3OH on Cu(110).

bidentate and unidentate formate species bonded to copper particles. They proposed the occurrence of the following reactions:

$$CH_3I_{(g)} + Cu \rightarrow CH_{3(ads)} + I_{(ads)},$$

$$CH_{3(ads)} + O_{(ads)} \rightarrow CH_3O_{(ads)},$$

$$CH_3O_{(ads)} + 3O_{(ads)} \rightarrow CH(O)_{2(ads)} + 2OH_{(ads)},$$

$$OH_{(ads)} + CH(O)_{2(ads)} \rightarrow H_2O_{(ads)} + CO_{x(ads)}$$
$$+ CO_{2(g)}.$$

As there was little spectroscopic evidence for the presence of adsorbed CH_3, it was assumed that C–I bond breaking and C–O bond making steps may be occurring either in a concerted fashion or very rapidly in a two-step process. Due to the high coverage of oxygen, methoxy can react further with adsorbed oxygen and subsequently dehydrogenate to form surface formate species, both bidentate and unidentate. They assumed that a methylenebis (oxy) $(CH_2(O)_2)$ species is a possible intermediate, although its existence was not observed.

4. Conclusions

Spectroscopic methods of surface science were found to be suitable tools to follow the primary interaction and reaction of hydrocarbon

Fig. 7. Infrared spectra of (a) oxidized Cu/SiO_2 after reaction with 15.0 Torr methyl iodide for 80 min at room temperature [60].
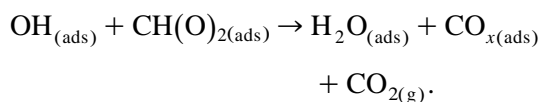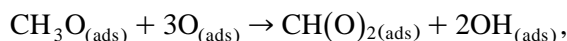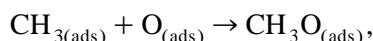
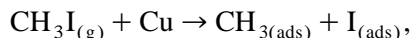fragments with adsorbed oxygen atoms on metal surfaces. Preadsorbed oxygen shifts the dissociation temperature of carbon–iodine bond cleavage in organic iodo compounds to higher temperatures. Hydrocarbon fragments formed combine readily with adsorbed oxygen atoms to yield oxygenated compounds. The product distribution of the oxidation reactions sensitively depends on the oxygen coverage which provides a possibility to direct selectivities in the catalytic oxidation of hydrocarbons.

Acknowledgements

References

[1] F. Zaera, J. Mol. Catal. 86 (1994) 221.
[2] F. Zaera, Acc. Chem. Res. 25 (1992) 260.
[3] B.E. Bent, Chem. Rev. 96 (1996) 1361.
[4] X.-L. Zhou, X.-Y. Zhou, J.M. White, Surf. Sci. Rep. 13 (1991) 73.
[5] A. Berkó, F. Solymosi, J. Phys. Chem. 93 (1989) 12.
[6] F. Solymosi, A. Berkó, K. Révész, Surf. Sci. 240 (1990) 50.
[7] J. Kiss, A. Berkó, K. Révész, F. Solymosi, Surf. Sci. 240 (1990) 59.
[8] F. Solymosi, J. Kiss, K. Revesz, J. Chem. Phys. 94 (1991) 8510.
[9] X.D. Peng, R. Wiswanathan, G.H. Smudde, P.C. Stair, Sci. Instr. 63 (1963) 3930.
[10] D. Jenz, M. Trenary, X.D. Peng, P. Stair, Surf. Sci. 341 (1995) 282.
[11] M.M. Hills, J.E. Parmeter, C.B. Mullins, W.H. Weinberg, J. Am. Chem. Soc. 108 (1986) 3554.
[12] F. Solymosi, G. Klivényi, J. Phys. Chem. 99 (1995) 8950.
[13] G. Klivényi, F. Solymosi, Surf. Sci. 342 (1995) 168.
[14] M.A. Henderson, G.E. Mitchell, I.M. White, Surf. Sci. 188 (1987) 206.
[15] C. Houtman, M.A. Barteau, Surf. Sci. 248 (1991) 57.
[16] F. Solymosi, J. Kiss, Surf. Sci. 149 (1985) 17.
[17] J.J. Zink, W.H. Weinberg, J. Vac. Sci. 17 (1980) 188.
[18] J. Kiss, F. Solymosi, Surf. Sci. 177 (1986) 191.
[19] F. Solymosi, J. Kiss, I. Koávcs, Surf. Sci. 192 (1987) 47.
[20] C.W.J. Bol, Friend, J. Am. Chem. Soc. 117 (1995) 11572.
[21] C.W.J. Bol, Friend, Surf. Sci. 331 (1985) L800.
[22] F. Solymosi, I. Kovács, K. Révész, Surf. Sci. 356 (1996) 121.
[23] F. Solymosi, I. Kovács, Surf. Sci. 296 (1993) 171.
[24] S.W. Jorgensen, R.J. Madix, J. Am. Chem. Soc. 110 (1988) 397.
[25] P.A. Thiel, T.E. Madey, Surf. Sci. Rep. 7 (1987) 211.
[26] E.M. Stuve, S.W. Jorgensen, R.J. Madix, Surf. Sci. 146 (1984) 179.
[27] F. Solymosi, A. Berkó, J. Catal. 101 (1986) 458.
[28] P. Berlowitz, B.L. Yang, J.B. Butt, H.H. Kung, Surf. Sci. 159 (1985) 540.
[29] X.-L. Zhou, Z.-M. Lin, J. Kiss, D.W. Sloan, J.M. White, J. Am. Chem. Soc. 117 (1995) 3565.
[30] I. Kovács, F. Solymosi, J. Mol. Catal. submitted.
[31] F. Solymosi, J. Kovacs, J. Phys. Chem. B 101 (1997) 5397.
[32] J.-L. Liu, B.E. Bent, J. Phys. Chem. 96 (1992) 8529.
[33] Ch.-M. Chiang, T.H. Wentzlaff, B.E. Bent, J. Phys. Chem. 96 (1992) 1836.
[34] I. Kovács, F. Solymosi, J. Phys. Chem., to be published.
[35] M. Bowker, R.J. Madix, Surf. Sci. 102 (1981) 542.
[36] B.A. Sexton, A.E. Hughes, N.R. Avery, Surf. Sci. 155 (1985) 366.
[37] J. Kiss, K.C. Smith, F. Solymosi, J.M. White, to be published.
[38] F. Solymosi, G. Klivényi, J. Electron Spectrosc. Relat. Phen. 64/65 (1993) 499.
[39] L. Bugyi, A. Oszkó, F. Solymosi, J. Catal. 159 (1996) 305.
[40] T.P. Beebe, J.L. Crowell, J.T. Yates Jr., J. Phys. Chem. 92 (1988) 1296.
[41] F. Solymosi, A. Berkó, T.I. Tarnóczi, Surf. Sci. 141 (1984) 533.
[42] F. Solymosi, T.I. Tarnóczi, A. Berkó, J. Phys. Chem. 88 (1984) 6170.
[43] C. Houtman, M.A. Barteau, Langmuir 6 (1990) 1558.
[44] J. Kiss, K. Révész, F. Solymosi, Surf. Sci. 207 (1988) 36.
[45] J. Kiss, F. Solymosi, Surf. Sci. 177 (1986) 191.
[46] J.J. Zinck, W.H. Weinberg, J. Vac. Sci. Technol. 17 (1980) 188.
[47] C.W.J. Bol, Friend, J. Am. Chem. Soc. 117 (1995) 8053.
[48] B.A. Sexton, G. Somorjai, J. Catal. 46 (1987) 167.
[49] J. Kiss, G. Klivényi, K. Révész, F. Solymosi, Surf. Sci. 223 (1989) 5551.
[50] F. Solymosi, A. Berkó, Z. Tóth, Surf. Sci. 285 (1993) 197.
[51] J.L. Davis, M.A. Barteau, Surf. Sci. 235 (1980) 235.
[52] X. Guo, L. Hanley, J.T. Yates Jr., J. Am. Chem. Soc. 111 (1989) 4605.
[53] I. Kovács, F. Solymosi, J. Phys. Chem. 97 (1993) 11056.
[54] F. Solymosi, I. Kovács, K. Révész, Catal. Lett. 27 (1994) 53.
[55] C.J. Hautman, M.A. Barteau, J. Catal. 130 (1991) 528.
[56] C.W.J. Bol, C.M. Friend, J. Phys. Chem. 99 (1995) 11930.
[57] N.R. Glason, F. Zaera, J. Catal. 169 (1997) 365.
[58] C.W.J. Bol, C.M. Friend, Surf. Sci. 364 (1996) L549.
[59] J. Raskó, I. Bontovics, F. Solymosi, J. Catal. 143 (1993) 138.
[60] M.D. Driessen, V.H. Grassian, J. Phys. Chem. 99 (1995) 16519.